Fitting DARKexp predictions to dark matter halo profiles from simulation

Chris Nolting

Submitted under the supervision of Liliya L. R. Williams to the University Honors Program at the University of Minnesota - Twin Cities in partial fulfillment of the requirements for the degree of Bachelor of Science, summa cum laude in Astrophysics.

May 8, 2014

Abstract

I performed analysis of dark matter halo data from the Millennium II simulation and fit the resulting energy and density distributions to the predictions of the DARKexp model. For halos near virial equilibrium, I found DARKexp to fit the simulated data well, supporting it as a theoretical model for the distribution of matter in galaxies. I also discuss the methods of data analysis and the Markov Chain Monte Carlo method used for fitting.

Background

To better understand the nature of galaxies, their structure, and how they might have formed, we want to understand how the matter in galaxies is distributed. However, current models for the distribution of matter in galaxies are purely empirical. They are fit functions that match the observations well, but have no theoretical base. The most commonly used empirical models for dark matter halos are the Navarro, Frenk, and White or NFW profile [2], and the Einasto profile [3]. The NFW profile has the functional form:

$$\rho(r) = \frac{\rho_0}{\left(\frac{r}{R_s}\right)\left(1+\frac{r}{R_s}\right)^2} \tag{1}$$

Where r is the radius in the galaxy, ρ_0 a scale factor for the density, and R_s is a scale distance for the galaxy. The distribution function is plotted below in figure 1.

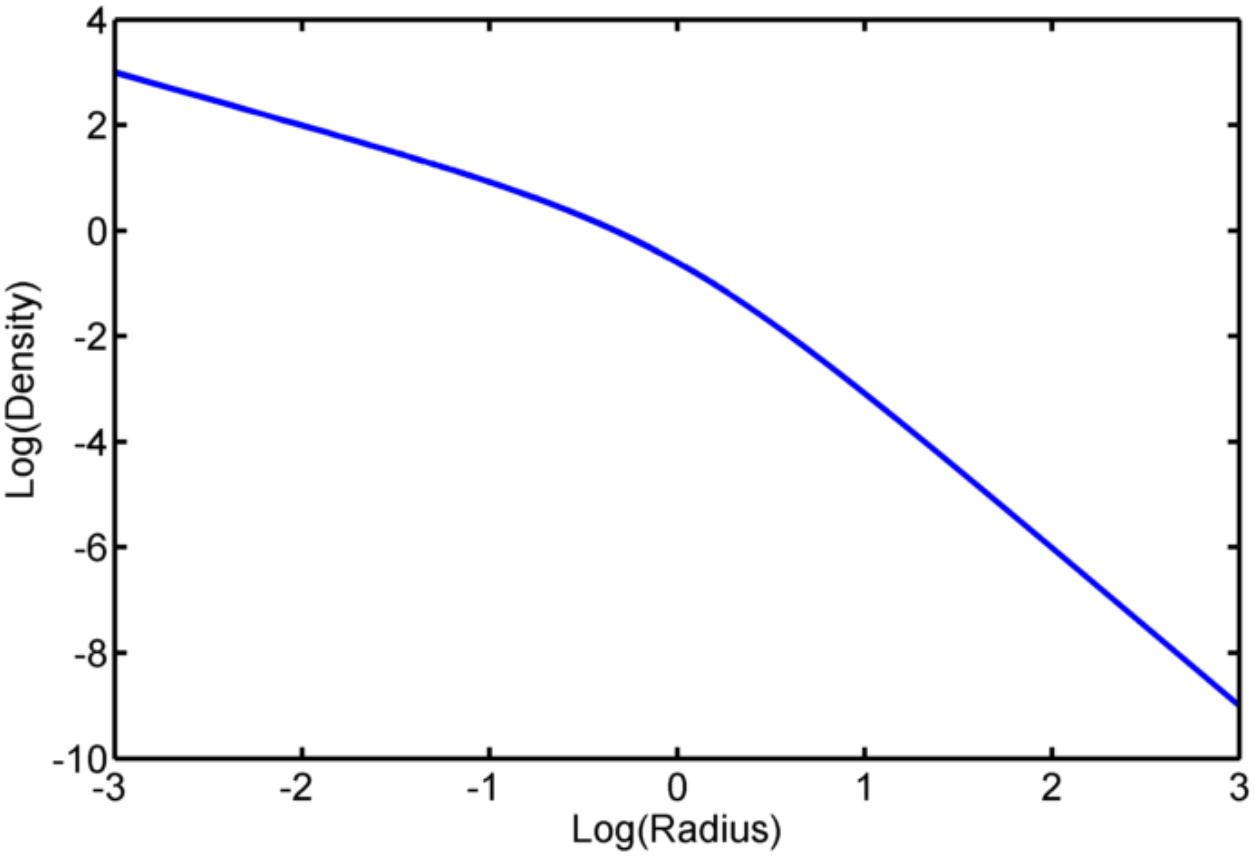

Figure 1: NFW distribution function plotted in Log(Radius) vs Log(Density).

NFW was a good fit for the early attempts at N-body simulation of dark matter halos, when the computational power required to run these simulations became available around the early 1990's [2]. The Einasto profile has the functional form:

$$\rho(r) = \rho_{-2} \exp\left(-\frac{2}{\alpha}\left[\left(\frac{r}{R_s}\right)^{\alpha} - 1\right]\right) \tag{2}$$

Where α is a shape parameter of the fit. Einasto's distribution is shown below in figure 2 for a various values of the shape parameter α.

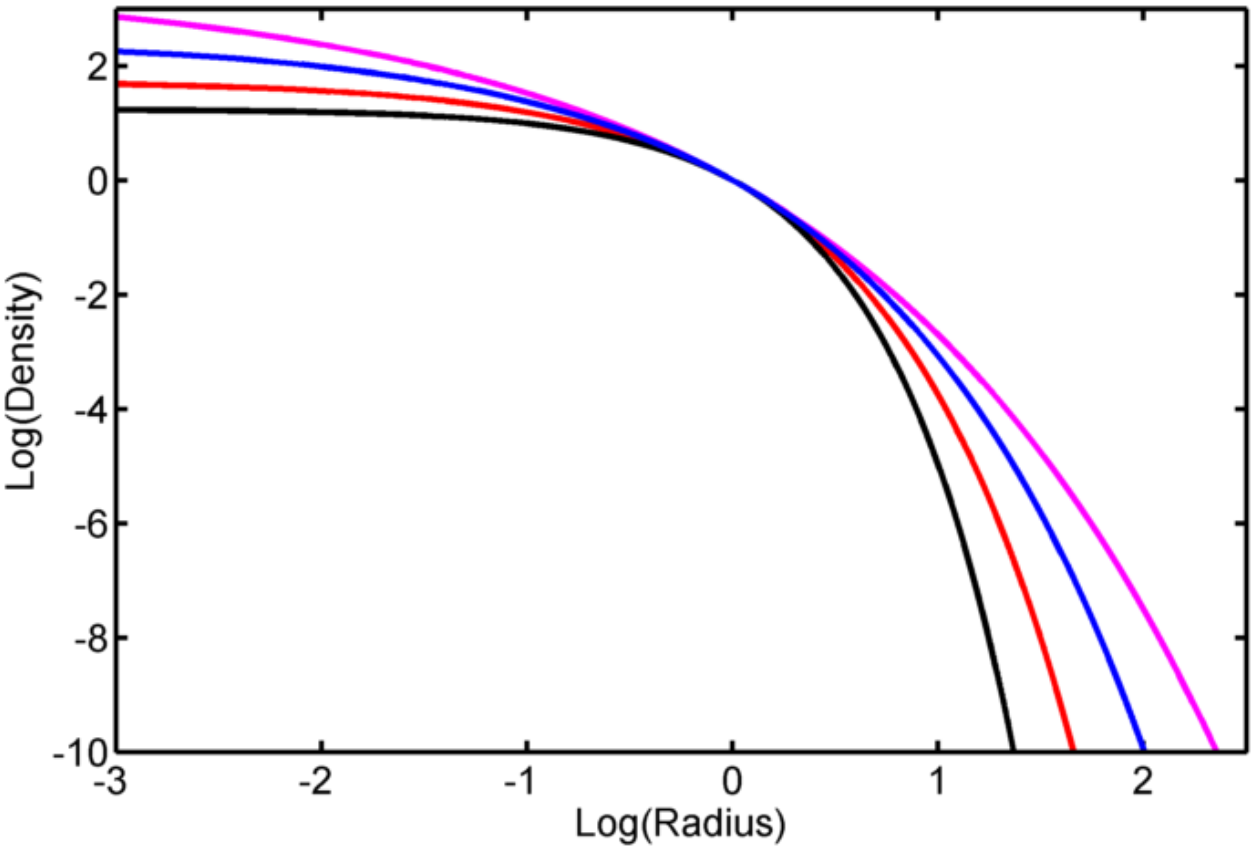

Figure 2: Einasto distribution function plotted in Log(Radius) vs Log(Density) for four values of the shape parameter α. Larger α corresponds to larger curvature. In magenta, $\alpha = 0.25$, in blue, $\alpha = 0.35$, in red, $\alpha = 0.5$, and in black, $\alpha = 0.7$.

Once computational power advanced further, and the resolution of numerical simulations increased, the Einasto profile was found to fit slightly better than NFW, although it was still purely empirical [4].

Starting from first principles, we would like to be able to predict the density and energy distributions for dark matter in galaxies. Numerical simulations tell us that the properties of dark matter halos are fairly universal, and depend little on the initial conditions of the system [5]. This means that there should be some underlying physics that would allow us to predict the distributions. Being able to do this would help us to check our understanding of how galaxies form and the processes that dominate galactic structure. The DARKexp theory takes a statistical mechanics approach and starts from a Boltzmann-like distribution and making a few modifications to the standard statistical approach. First, DARKexp

contends that the natural way to partition state space is in energy space, not in phase space. This is because in a collisionless system such as a dark matter halo, the particles are orbiting and only interacting with the global potential. In such a system, once equilibrium is reached, each particle will retain its total energy. The second major change introduced by the DARKexp theory is the way that small occupation numbers are handled. For well bound particles (those with very negative potentials) the number of particles in that energy range can be very small. The way that DARKexp handles these low occupation numbers effects the density profile at the inner-most portion of the halo.

Besides the DARKexp theory, a few other groups have tried to come up with theoretical models in the past, with some success. In 2013, Beraldo et al. tested a selection of theoretical and empirical distribution functions against data from real galaxy clusters. Of the theoretical distributions, DARKexp fit the data best, even beating out many of the empirical fits [6]. DARKexp predicts an energy distribution of the form:

$$N(\varepsilon) \propto \exp(\phi_0 - \varepsilon) - 1 \tag{3}$$

or

$$N(E) = A * [\exp(\beta(\Phi_0 - E)) - 1] \tag{4}$$

Where in (4), A is a scale factor on the total number of particles per energy interval, β is the inverse temperature scale factor for the energy, Φ_0 is the potential at the center of the halo, and E is the total energy of the particle (Kinetic and Potential). In (3), $\phi_0 = \beta * \Phi_0$ and $\varepsilon = \beta * E$ are the dimensionless scaled central potential and dimensionless scaled particle energy respectively. To continue to test the DARKexp theory, I compare the predictions for the energy and density distributions to those derived from large N-body simulations by fitting using a Markov Chain Monte Carlo technique.

Simulation

The data used came from the Millennium II simulation from the Max Planck Institute for Astrophysics in Garching, Germany*. The Millennium II simulation was a large N-body simulation of large scale universal structure. The total size of the simulation was 100Mpc wide with a special resolution of 1kpc†. Each particle in the simulation had a mass of $6.885\,10^6 M_\odot$ [7]. The overall simulation tracked 10^{10} particles and contained many structures to be separated into 'galaxy halos.' To separate one 'galaxy halo' from another in the simulation, a friends-of-friends method was used [8]. This method required a scale length and a starting particle. All particles in the simulation within the scale length of the initial particle were labeled 'friends' and thus were part of the same galaxy halo. Then, from each 'friend' particle, all particles within the scale length of the 'friend' were also labeled 'friends.' This process was repeated for every particle that was labeled a 'friend' until there were no more particles within the scale length of any particle labeled a 'friend.' These collections of particles were considered distinct dark matter halos. Figure 3 below shows the total scale of the simulation, then zooms in repeatedly until a single friend-of-friend halo is visible.

*Mike Boylan-Kolchin supplied the data to my advisor, Liliya Williams

†Many parameters in the simulation have a dependence on the hubble parameter.
Ex: $\frac{Mpc}{h}$, $\frac{M_\odot}{h}$. I omit the hubble parameter for simplicity and will do so throughout this paper.

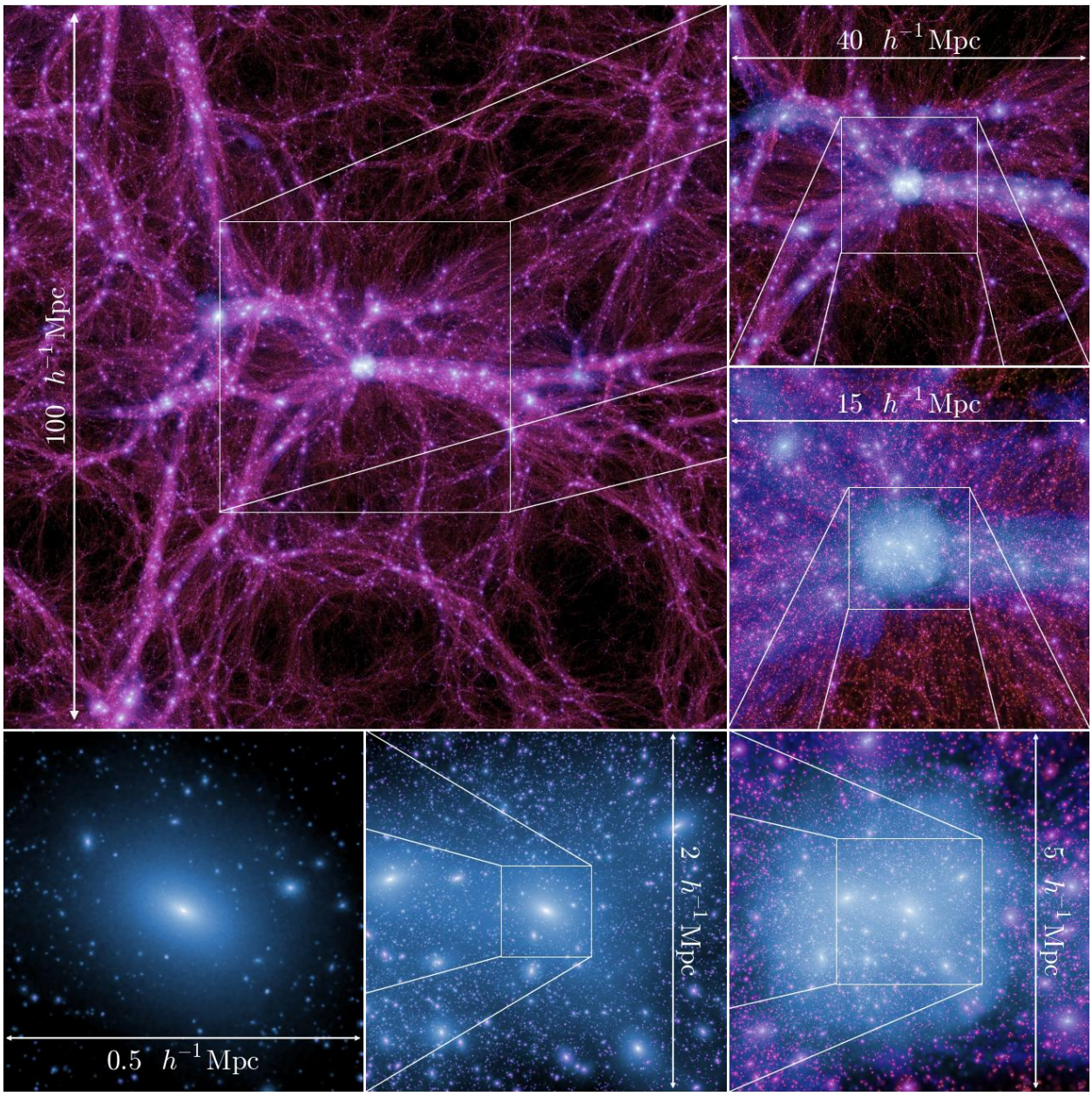

Figure 3: Millennium II N-body simulation, beginning at the total scale of the simulation and zooming in repeatedly to one friend-of-friend halo object. The simulation is 100Mpc across, while an individual halo object is on the order of 0.5 Mpc across

Data

The data sets contained the positions and velocities in the three coordinate directions as well as the specific potential (potential per unit mass)[‡] for each particle in the halo. Each halo had between 10^5 and 3.5×10^5 particles, corresponding to a total mass near $10^{12} M_\odot$ for the halos. I received 10 halo data sets initially in June 2013 and then ten additional data sets in March 2014. These additional data sets were from a larger mass range (about 10x mass), so to maintain a reasonable file size, only every 10th particle from the simulation was included.

Analysis

I ran many different types of analysis on the data. In order to generate the density and energy distributions from the simulated data, the data had to be binned in three ways: linearly in radius, logarithmically in radius, and linearly in energy. For the linear radius bins, the total radius of the halo was divided into 500 evenly spaced bins. The logarithmic radius binning divided this total radius into 500 bins, each bin 1% larger than the previous bin. The linear energy binning took the minimum and maximum total energies and divided the range into 200 evenly spaced bins. The energy distribution had fewer bins to reduce the Poisson noise and smooth the distribution when plotting and fitting.

Before determining the values for the particles' radii, the positions of the halo particles had to be shifted to re-center the coordinate system on the halo being analyzed. This was necessary since the positions given were taken from the larger simulation, so correspond to the particle's position in the 100Mpc cube. The original ten data sets were ordered such that the first particle in the set was the 'center' of the halo. In these cases, I originally subtracted the first particle's position from each other particle's position to re-center the particles. This was not always the case for later data sets, however, so the central particle was taken to be the particle in the data set that was at the deepest (lowest or most negative) potential, and

[‡]From now on I will not use the word 'specific,' however when I refer to an energy, I will always be talking about energy per particle mass

I subtracted off this particle's position to re-center all halos (including the original ordered sets).

To find the energy of the particles, I had to find the particles' velocities relative to the rest of the halo. To do this, the bulk motion of the halo through the rest of the simulation was subtracted off. This bulk motion was found by averaging the velocities of the inner-most particles of the halo[§]. After subtracting off this bulk motion, the kinetic energy was recorded for each particle. To find total energy, however, the potential is needed. The Millennium II data had values for the potential of each particle, but because the larger simulation had other particles contributing to the potential of every particle and because of other effects such as taking into account the expansion of the universe (Hubble flow), the potential values provided to me had some constant shift associated with them. This shift became extremely obvious when some halos had many particles with positive potentials. By its definition, the potentials should never be positive, and should become more and more negative deeper inside the halo. To avoid this issue, I decided to to calculate the potential values directly.

Given the exact positions of the particles,the potential at any point mass can be determined by finding the distance to every other point mass in the system. The potential is given by

$$\Phi_i = \sum_{i \neq j} -\frac{G\, m_j}{r_{ij}} \tag{5}$$

Where r_{ij} is the distance between the i^{th} and j^{th} particles and m_j is the mass of the j^{th} particle[¶]. The general agreement between the Millennium II potentials and the calculated potentials distribution shapes can be seen in figure 4 below.

[§]Inner-most meaning particles with a radius less than 7% of the maximum radius. This value was taken such that this contained about the inner-most 10% of particles for most halos.

[¶]For the large halos with $\frac{1}{10}$ sampling rate, each particle was assigned 10 times its normal mass

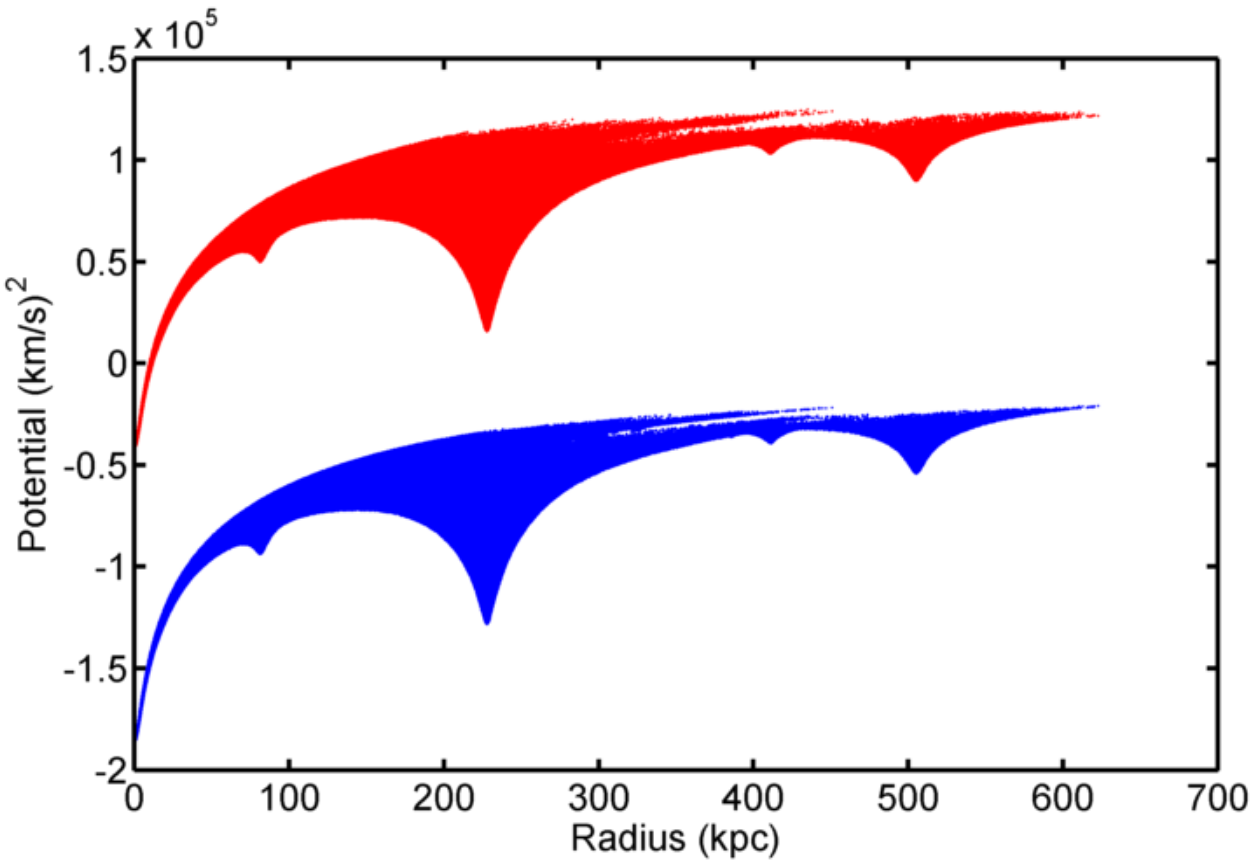

Figure 4: In Red: Millennium II potential of each particle for halo 1594
In Blue: Calculated potential of each particle for halo 1594

Figure 4 shows that the constant shift has effectively been removed by directly calculating the potential values, and now no particle resides at a positive potential value.

To better see the shape of the potential distribution, the potential was averaged, spherically outward using the linear radius bins. This helped because the density of points when plotting the potential as a function of radius for each particle was very high, creating dense, difficult to read plots. By averaging the potential of all points in a given bin, the plots became easier to read. Figure 5 below shows the spherically averaged potential for halo 1594.

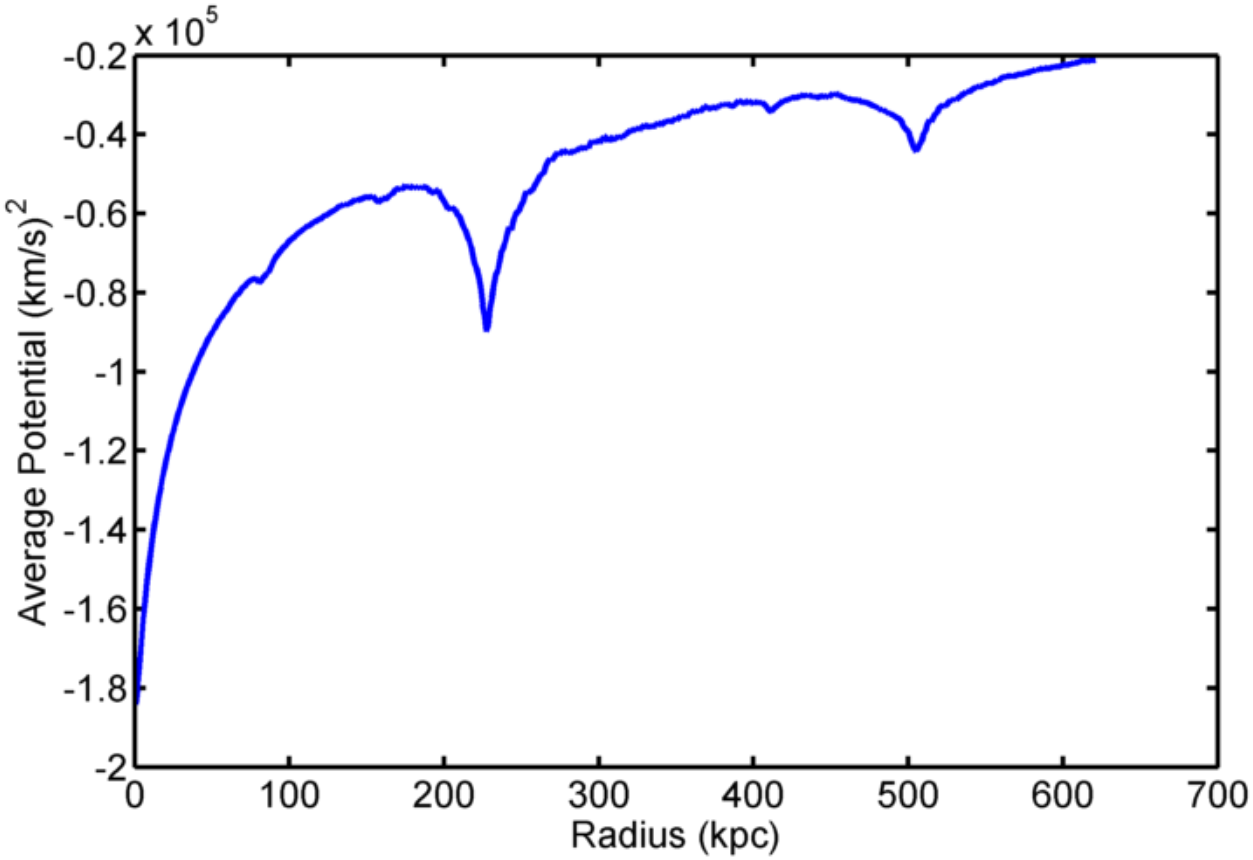

Figure 5: Spherically averaged (calculated) potential for halo 1594. Substructures embedded within the halo can be seen as dips in the potential.

The same general shape from figure 2 remains, however now the effects of substructures embedded within the halo have been lessened and it is easier to see the natural shape of the potential vs radius curve.

As a check, the difference between the Millennium II potentials and the calculated potentials was plotted against particle radius. In figure 6, it can be seen that for the most part, there is just a constant shift between them, with some scatter.

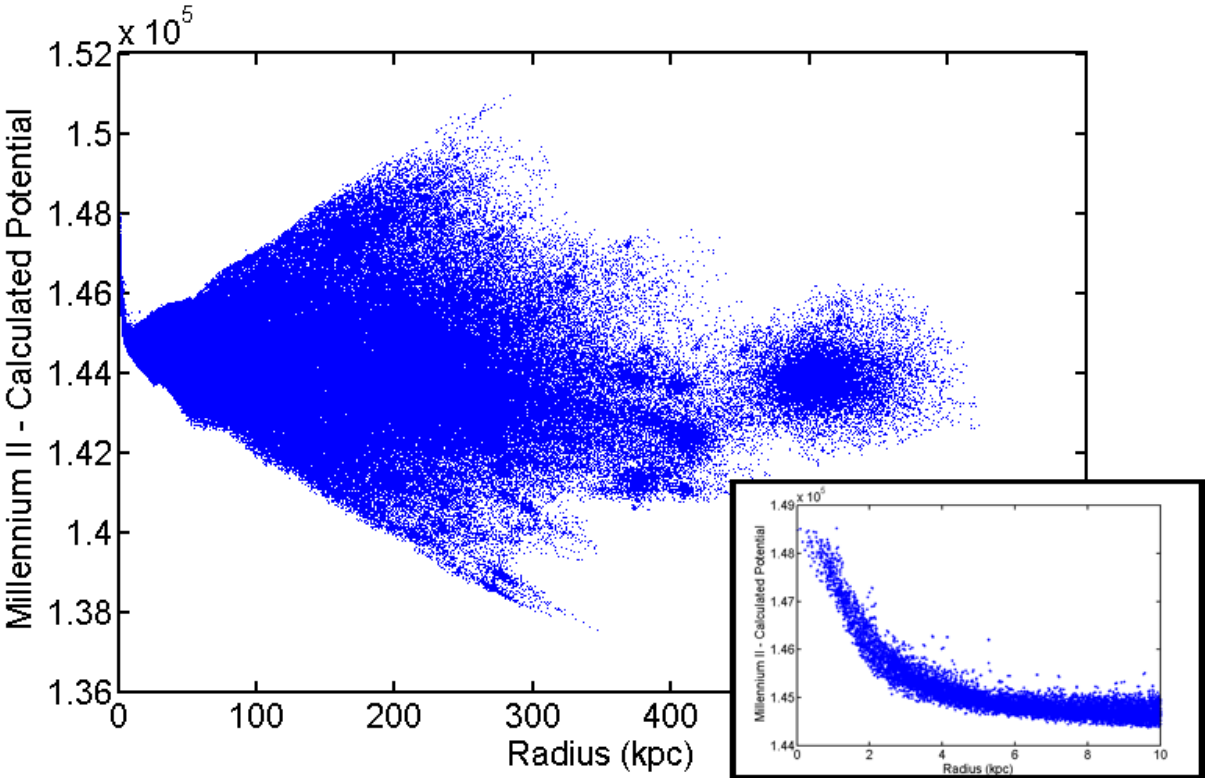

Figure 6: The difference between the Millennium II potential and the calculated potential is shown. Also shown is a zoom on the inner-most portion to showcase the upturn at the center of the halo.

Two important things can be seen in figure 6. First, as one would expect, the scatter in the difference between Millennium II and direct calculation grows larger the farther away from the center of the halo you go. This is because those particles are closer to other particles in the simulation that contribute more to their potential values in Millennium II, but are not taken into account in the calculated potential values because they are not in the same halo. The second thing to notice is that in the center of the halo (or in fact the center of any sub-structure as well) the Millennium II potential values are 'shallower' or larger than when calculated directly. This was due to a 'smoothing' of the potential which was done by Millennium II when calculating their potentials. The smoothing procedure involved a kernel

from Springel 2001[9]. The form of the kernel was:

$$W_2(u) = \begin{cases} \frac{16}{3}u^2 - \frac{48}{5}u^4 + \frac{32}{5}u^5 - \frac{14}{5} & : 0 \leq u < \frac{1}{2} \\ \frac{1}{15u} + \frac{32}{3}u^2 - 16u^3 + \frac{48}{5}u^4 - \frac{32}{15}u^5 - \frac{16}{5} & : \frac{1}{2} \leq u < 1 \\ -\frac{1}{u} & : u \geq 1 \end{cases} \tag{6}$$

Using this kernel, the potential calculation from (5) was modified to be:

$$\Phi_i(r_{ij}) = G\,\frac{m}{h}\,W_2\left(\frac{r_{ij}}{h}\right) \tag{7}$$

Here h is some scale length, which was 2.8kpc in the Millennium II simulation[10]. This change acts as a 'force softening' that prevents large scattering angles in numerical simulations. This is an important part of dark matter simulations, in which the particles are assumed to interact only with the global potential and not feel the effects of their nearest neighbors. The effect of the kernel is that at small particle separations, the contribution to the potential becomes a constant value, and thus there is no gradient in the potential for particles very nearby. With no gradient in the potential, the particle feels no gravitational force, preventing scattering due to local particles. With this modification to the calculation of the potential, the up-turn from figure 6 disappeared.

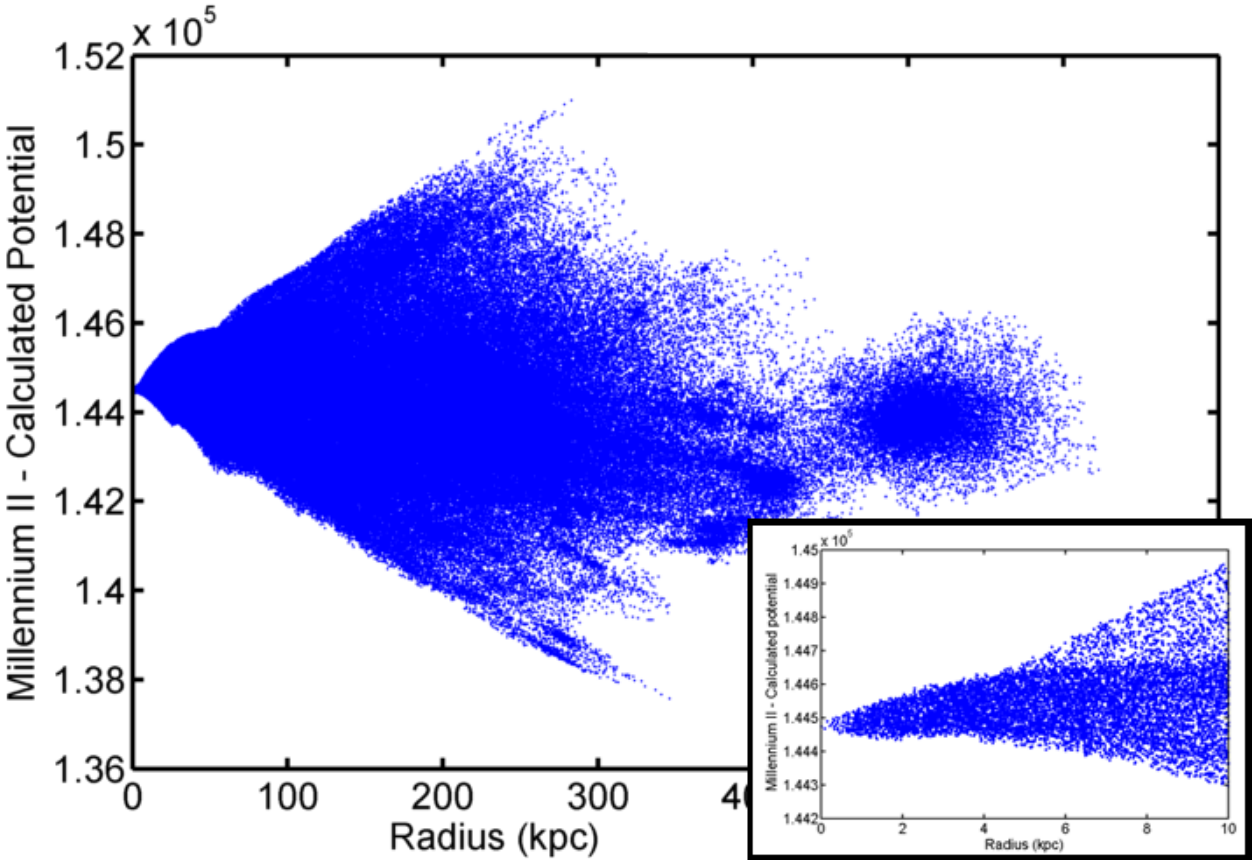

Figure 7: Millennium II - Calculated Potential vs radius using W2 Kernal from equation (6). The central turn-up has been removed using the smoothing kernal.

These potential values were used to find the total particle energy and in all subsequent data analysis.

Determining Equilibrium

If a 'halo' is out of equilibrium, the predictions of DARKexp do not apply, due to assumptions made in the derivation of the distribution function. Also, many forms of analysis used thus far are based on the idea that the 'halo' is at least near to virial equilibrium. Because of this, it was very important for me to check to see that the halos I had received were in fact in equilibrium. In order to check this I examined two things: the virial ratio for the halo and the position projections of the particles, looking for evidence that the halo is out of equilibrium.

With values for the potential of each particle, and the edges of the bins defined, the virial ratio could be calculated as a check on how well relaxed or 'virialized' the halos were. The virial ratio is defined as:

$$\text{Virial Ratio} = -\frac{\sum_{\text{i}}^{\text{N}} \text{K}_{\text{i}}}{\sum_{\text{i}}^{\text{N}} \Phi_{\text{i}}} \tag{8}$$

Where K_i and Φ_i are the kinetic energies and potential energies of the i^{th} particle, respectively. Ideally, if the halo was completely in virial equilibrium, this value would be 1/2 after summing over the entire halo. This sum is cumulative outward from the center. Using the linear radius bins, the total kinetic energy and the total energy of all particles within the current bin (as well as any previous bins) were summed separately, and then the negative ratio of the total kinetic to the total potential energy was recorded. A plot of the virial ratio for halo 1594 vs radius is shown in figure 8 below.

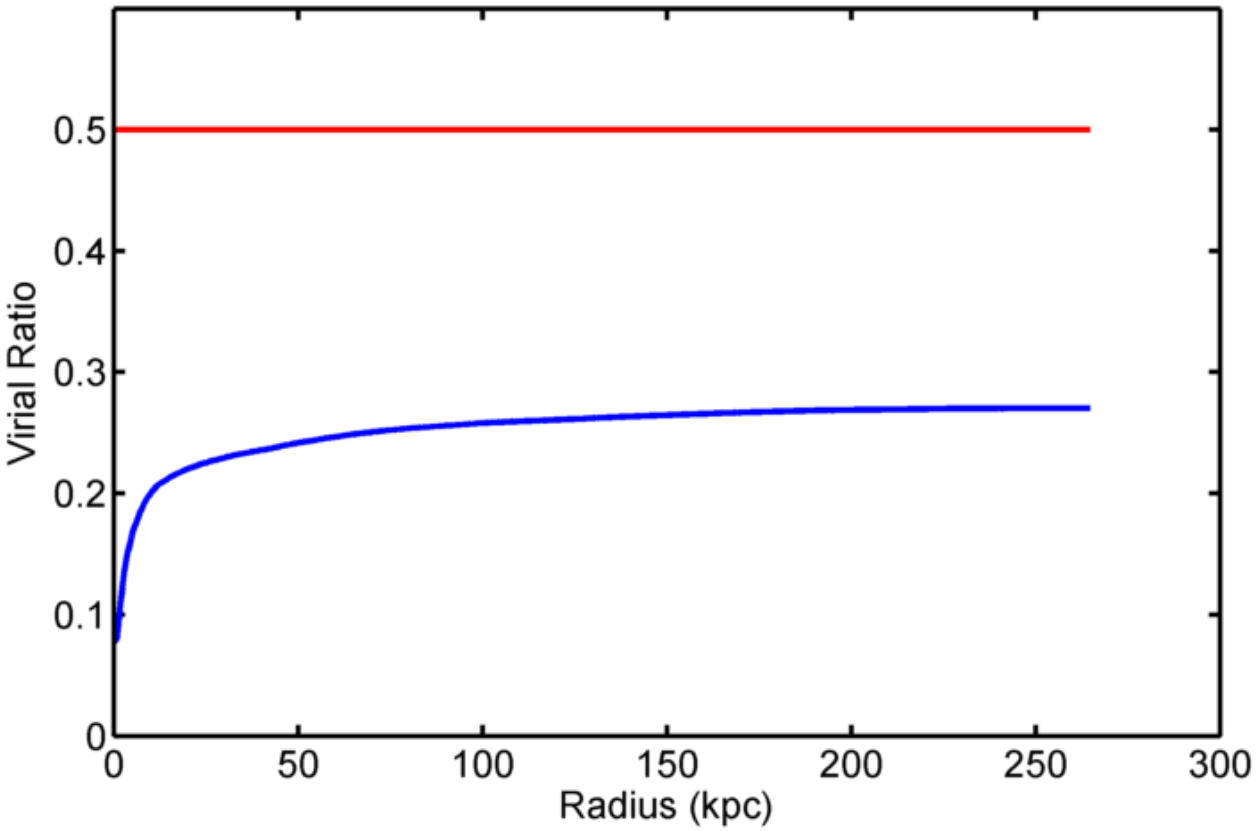

Figure 8: Cumulative virial ratio, integrated outward from the center for halo 4090, in red the expectation for virial equilibrium, 0.5, is shown. The virial ratio asymptotically approaches a value near 0.3, which appears to be characteristic of halos I received near equilibrium.

As can be seen in figure 8, the virial ratio in the center of the halo begins very small, as these particles have very negative, deep potentials. At larger radii, when nearly the entire halo has been summed, the virial ratio approaches a value near 0.3 asymptotically. This seems to be characteristic of the data for halos that I received near virial equilibrium. If a system is far from equilibrium, then we will see that in the virial ratio, which often exhibits 'steps' in the virial ratio at certain radii, where the virial ratio increases noticeably over a short range rather than rising smoothly to a constant asymptotic value. This can be seen in figure 9 below in which the plot of the virial ratio vs radius for 'halo' 232 is shown.

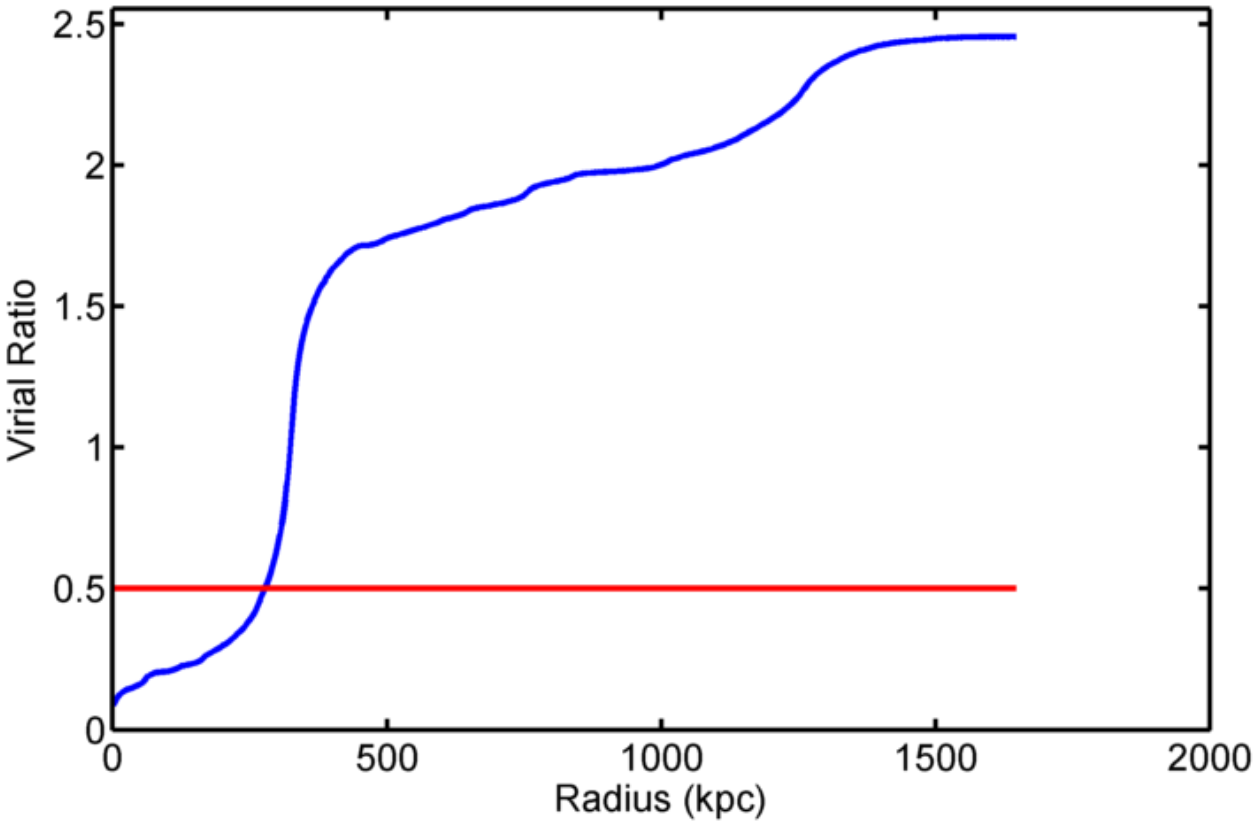

Figure 9: Cumulative virial ratio, integrated outward from the center for halo 232, in red the expectation for virial equilibrium, 0.5, is shown. The virial ratio jumps drastically to large values, indicating that the 'halo' is still in the process of merging and is not in equilibrium.

This structure is clearly not in any kind of virial equilibrium; its kinetic energy is far too high, causing the virial ratio to be much more than 0.5. When we look at the plots of the particles' positions in three dimensions, we can see what is happening. Below in figure 10, three projections of the three dimensional positions are shown.

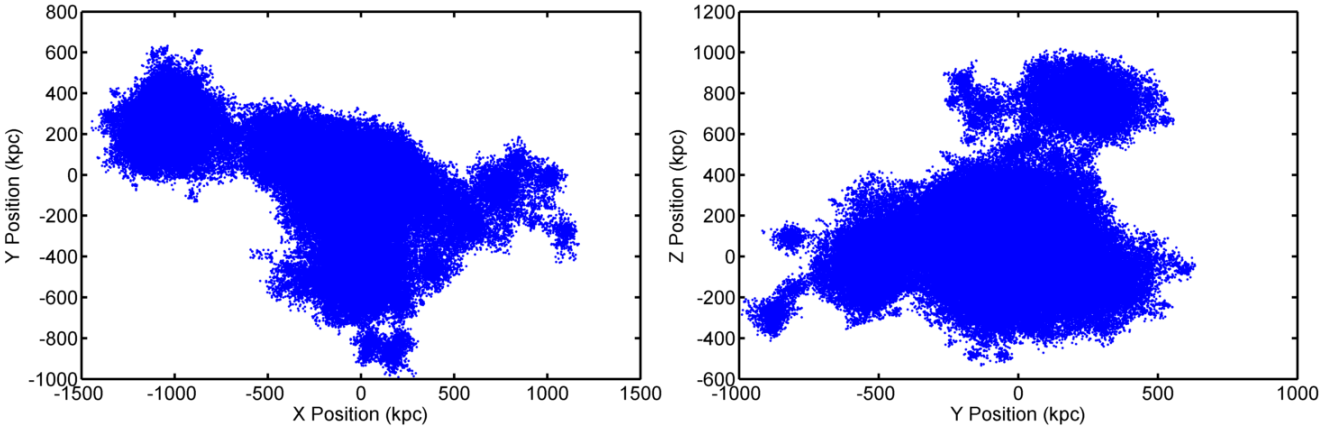

(a) x-y positions

(b) y-z positions

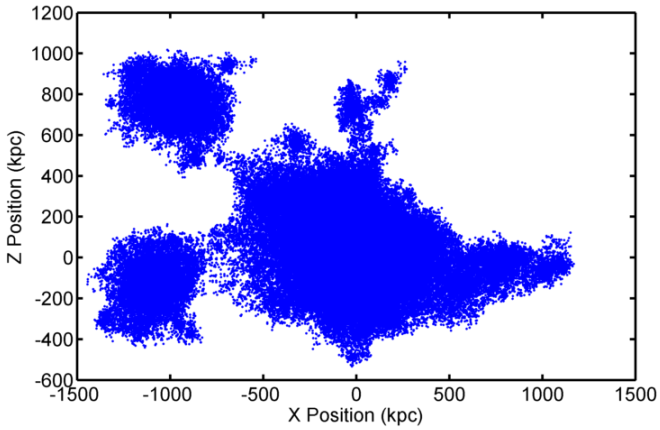

(c) x-z positions

Figure 10: Three projections of the positions for particles in halo 232. It can be seen that there are mulitple structures still in the process of merging together, and that the 'halo' is not in equilibrium.

Figure 10 gives another method of determining that this structure is not in equilibrium. It appears to be at least three separate structures still in the process of merging together. Since it is not relaxed, the predictions of DARKexp do not apply and it is not expected that it will give a good fit for the density and energy distributions. Using the corresponding plots to figures 8 and 10 for each halo, it was determined weather or not the halo was in equilibrium, and to use the the data in analysis or to ignore it.

Fitting Techniques

Once the data analysis was complete, it was time to fit the data to the DARKexp theory. The process I used to fit was a Markov Chain Monte Carlo technique. This technique 'steps around' in a parameter space for an area of low RMS (Root Mean Square) deviation from the model. Markov Chain methods mean that the future state of the system depends only on the current state of the system, and not on the history of the system. In my fitting method, this means that the next 'step' depends only on the current RMS and associated fitting parameters, and not on the previous RMS or parameter values. This, along with an added 'pressure' that pushes toward low RMS values, enables the fitting technique to find areas of low RMS as it 'steps' randomly through the space.

Density Profile Fitting

Since the density profile for the DARKexp theory is analytically unsolvable, I was provided with finely spaced numerically calculated values by my advisor, Liliya Williams[‖]. Comparing to these calculated values for the logarithm (base 10) of the density and the logarithm of the radius, I found the RMS[**] for the log density profile derived from the simulated data. The data was scaled such that the log radius and log density values overlapped with the numerically calculated DARKexp data sets. The scale factors used were 10^3 and 10^{-18} for radius and density respectively. After I scaled the data and took the logarithm, a Gaussian random number, centered at zero and scaled by some constant value, was generated and added to the log density values taken from simulation. The same was done for the log radius, with a different scaling constant. Gaussian random numbers were generated using the Box-Muller transform:

$$N = \sqrt{-2 \ln x_1} \cos(2\pi x_2) \tag{9}$$

[‖] These values are published on her personal website http://homepages.spa.umn.edu/ llrw/DARKexp.html

[**] RMS calculation techniques are given in Appendix A

Where x_1 and x_2 are two independent random numbers from a uniform distribution (0,1]. Together, these two shifts corresponded to a random 'step' in the two parameter fitting space. Then, the RMS was checked again after the simulated values were shifted. If this new RMS was lower, the 'step' was taken, and the parameter values and RMS were recorded. If the new RMS was worse, the probability that the step would still be taken would be given by:

$$\text{Probability}(\text{n}^{\text{th}}\text{step}) = \exp\left[-\left(\frac{\text{RMS}_\text{n}}{\text{RMS}_{\text{n}-1}}\right)^2\right] \tag{10}$$

Where RMS_n is the new RMS after the n^{th} step (if it is taken) and RMS_{n-1} is the previous RMS at the location in the parameter space before the step to be taken. Equation (10) makes it so that the probability of taking a step that is toward a larger RMS decreases quickly if the RMS is much worse than previously. If the RMS is only slightly worse, $\frac{RMS_n}{RMS_{n-1}}$ will be close to 1, so the probability will be near 1/e $\approx$ 37%. If the step was not taken, the shift was not applied, and a new random 'step' was generated. This process repeated until 1000 steps had been successfully taken. This lead to a minimum RMS value, after a pseudo-random walk through the two parameter space. In figure 11, the value of the RMS deviation vs step number and the walk through the parameter space are shown.

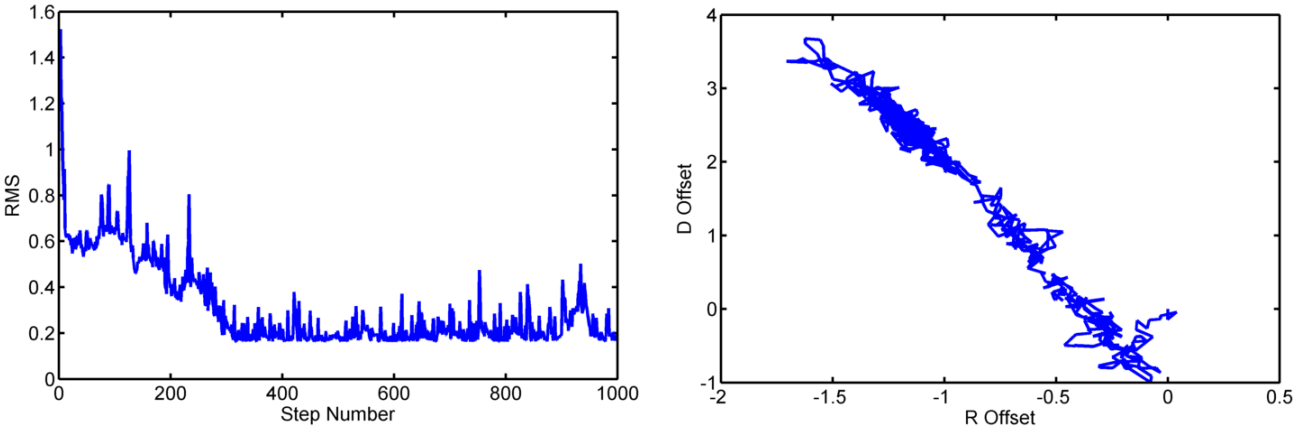

(a) RMS for each step in the fitting process

(b) Walk through two parameter fitting space

Figure 11: Density Fitting Process for halo 4090 with $\phi_0 = 3.0$

Over the course of the fitting process, the lowest value for the RMS deviation and corresponding parameters were recorded. These values were used when plotting the final fits. For each halo, this process was repeated for different values of the halo potential depth parameter ϕ_0, which changes the shape of the numerically calculated density distribution. This in effect adds a third fitting parameter, because one value of ϕ_0 will give the lowest RMS, and best fit for the halo. The density distribution for halo 1594 is shown below in figure 12, along with the best fitting DARKexp prediction.

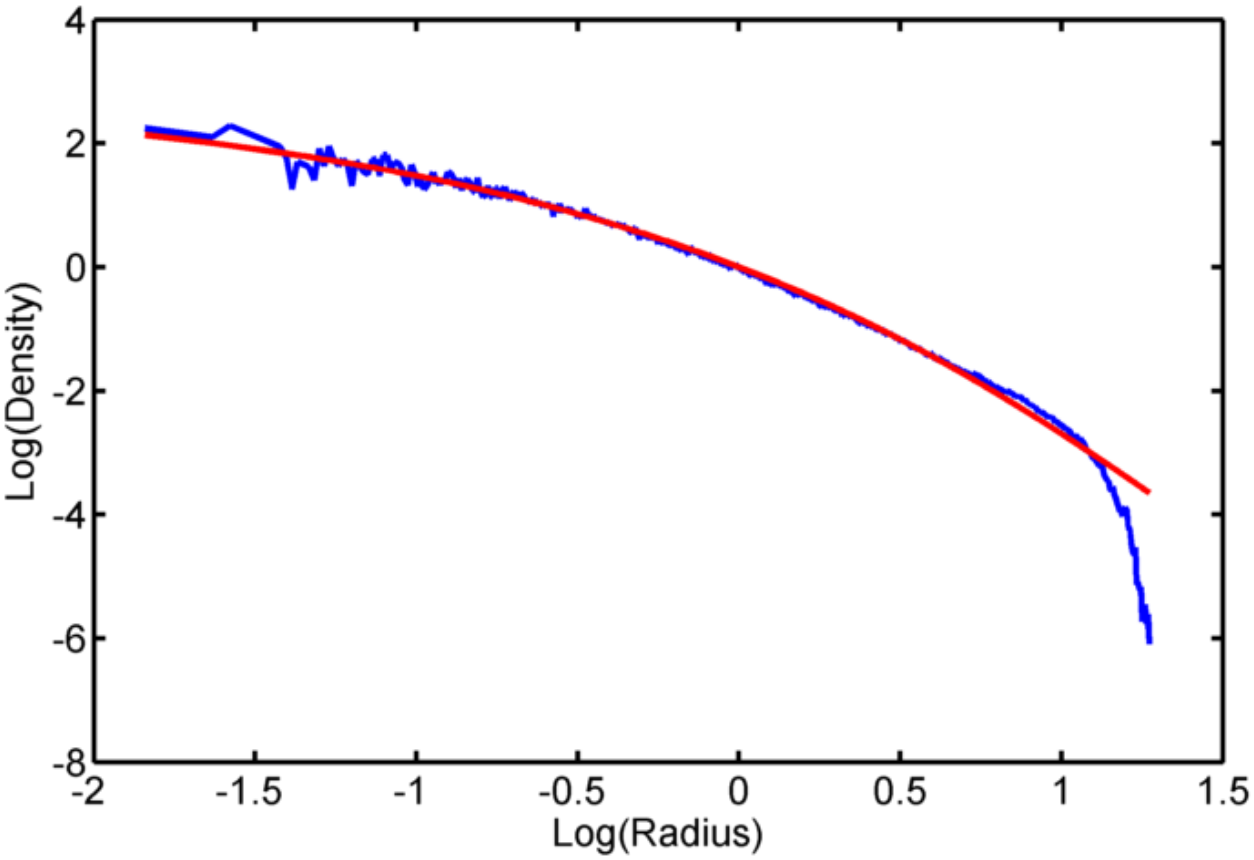

Figure 12: Final density fit for halo 4090, using $\phi_0 = 3.0$ and with R_{offset} = -1.149255 and D_{offset} = 2.431115

Local Minima

Markov Chain Monte Carlo techniques can be used to avoid getting trapped in areas of the two parameter space that correspond to local minima for the RMS. By generating Gaussian random steps using equation (9), it is possible to get large steps as big as a few times the

step size scale factor. This possibility for large step sizes allows this technique to escape local minima for the RMS and seek out the global minima for the parameter space. Also, by using equation (10) for the probability of taking a step, it is possible for the fit to take a step that is toward 'worse' RMS, and can climb out of a local minima and seek the global minima.

Energy Profile Fitting

A similar process to the density fitting was used to fit the energy distribution. Since the DARKexp theory predicts an energy distribution of:

$$N(E) = A * [\exp(\beta(\Phi_0 - E)) - 1]$$

As in equation (4), we can compare to this model rather than numerically calculated values. Instead of 2 fitting parameters, as in the density fitting procedure, there are now three fitting parameters: A, β, and Φ_0. The fitting is started with some reasonable values[††], and uses the same Markov Chain Monte Carlo fitting method to take random steps through a now three-dimensional space. Equation (10) was used again for the probability of taking a step if the new RMS was larger than the RMS before the step. In the case where the model extended beyond the data, additional bins were added until the fitted model predicted zero particles (at deepest particle potentials). Each additional bin contained zero particles since no simulated particles were at those energies. Below in figure 13, the results of fitting the energy distribution of halo 4090 are shown.

[††]The scale factor A have given an original value of 1 (no scaling), Φ_0 took the value of the center of the minimum energy bin, and β was originally -10^{-5} to scale the energies down

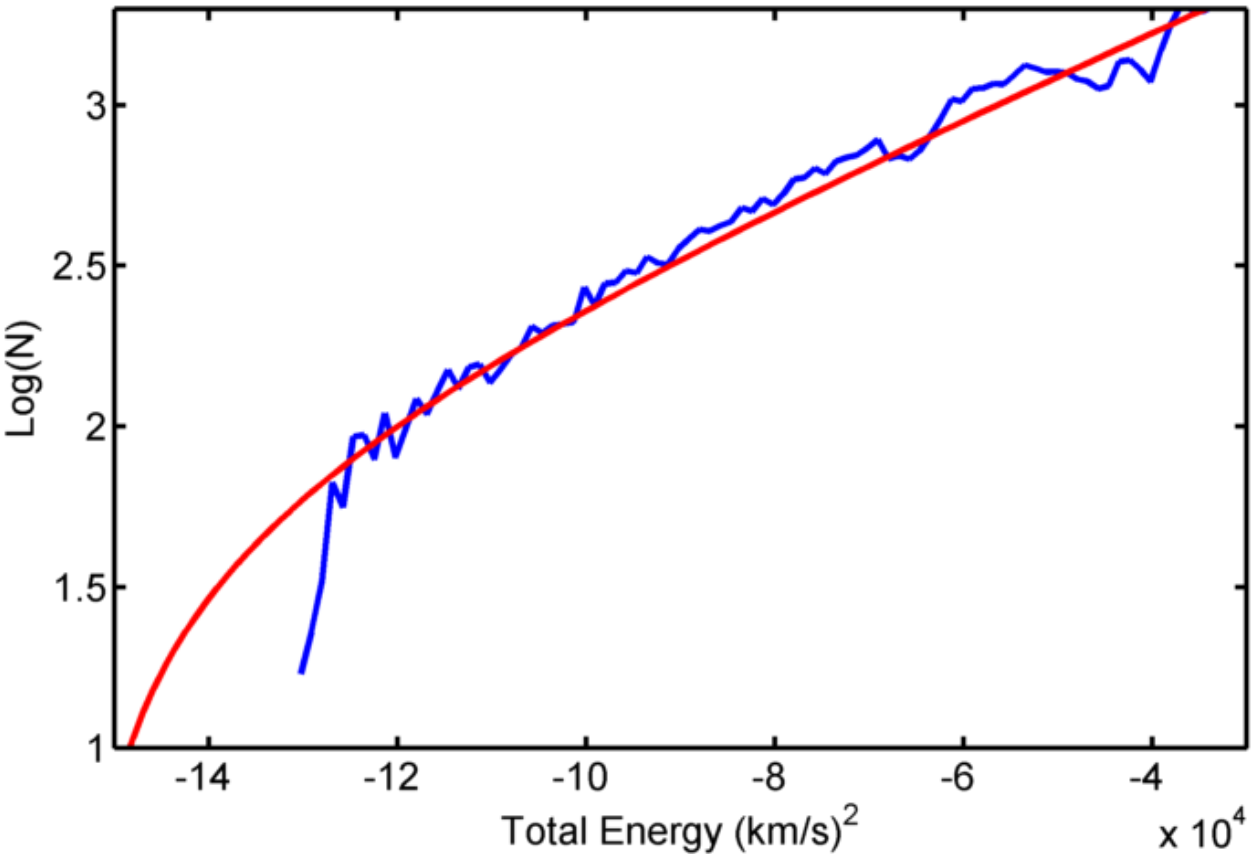

Figure 13: Energy distribution and DARKexp fit for halo 4090, using Φ_0 = -153749.5, β =-0.000030, and $A = 10^{1.755832}$.

Discussion

From the density distribution, in figure 12, we can see that the density profile fits very well for most of the range, and only deviates at large radii. This could be in part due to the friends-of-friends method used to separate the 'halo' object from the simulation at large. This process could be missing some of the particles associated with the halo that are farther out and not as densely packed, so are far enough away from their neighbors that they are not included as 'friends' by the method. Since it is necessary to say that some particles are members of one halo and not another, a cut must be made and there will be losses at large radii.

From the energy distribution in figure 13, we can see that the prediction of DARKexp fits

the data well outside of the central regions, where it predicts too many particles. However, this mostly shows up in the log plot. As we can see in the linear plot in figure 14 below, this is not as large a deviation as it may seem.

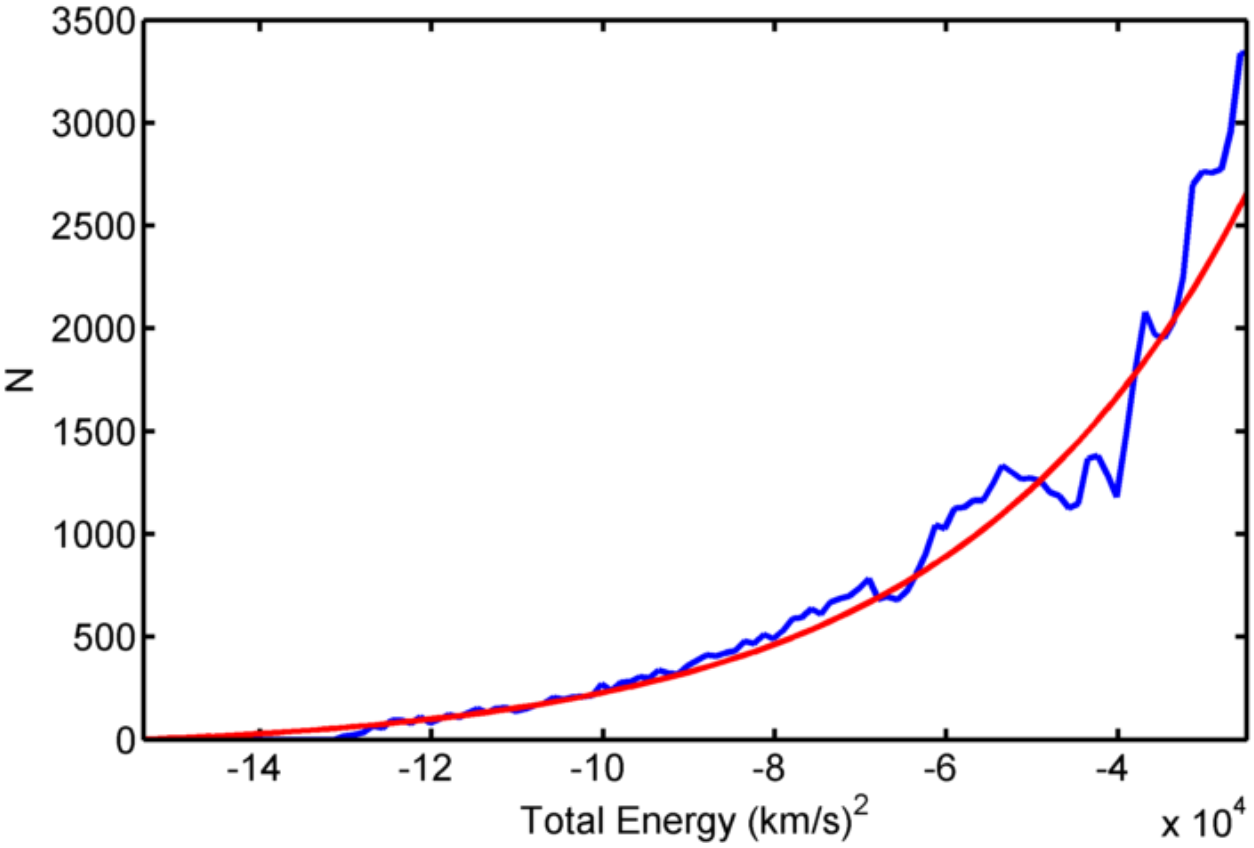

Figure 14: The same fit as figure 13, but in linear space. The fitting was done on N, not log(N), so this best represents the fit, however the log space is easier to look at in most cases.

Conclusions

For those halos found to be close to being considered 'relaxed' as discussed above, DARKexp was found to consistently fit the data from Millennium II well. For those halos that were not 'relaxed,' DARKexp is not expected to fit the data, as it assumes that the system is in the final equilibrium state, derived from the highest entropy state of the system[1].

We have seen that DARKexp provides a good fit to the energy and density distributions of dark matter in simulations. Beraldo et al. (2013) found that DARKexp fit data

from galaxy clusters as well as the tested empirical models[6]. This lends support to the theoretically based model, DARKexp, to describe the distribution of dark matter in galaxies.

Acknowledgements

I would like to thank the following people for their help and contributions to my thesis work:

Liliya Williams my advisor, for working with my for the last year and helping me to confront the problems that I encountered.

Mike Boylan-Kolchin for supplying me with the data from the Millennium II simulation and for answering questions about the simulation parameters and potential calculation processes and density smoothing kernals.

Cord Labarre for help in the initial coding of the data analysis program, and for helping to parallelize the direct potential calculation program.

Mike Veit for helping me to generate the plots used in this work.

Terry Jones and Jeremiah Mans for being my additional thesis readers.

Appendix A: RMS Calculations

Density Fitting

$$RMS = \frac{\sum_i^{500} |\log[\rho(i)] - \log[\rho_{theory}(i)]|^2}{\sum_i^{500} \sqrt{N(i)}}$$

Where we are summing over 500 bins. $\log[\rho(i)]$ is the density from simulation, $\log[\rho_{theory}(i)]$ is the density numerically calculated from DARKexp predictions by my advisor Liliya Williams, and $N(i)$ is the number of simulation particles in that bin.

Energy Fitting

$$RMS = \frac{\sum_i^n |[N(i) - N_{theory}(i)]|^2}{\sum_i^n \sqrt{N_{theory}(i)}}$$

Where $N(i)$ is the number of simulated particles with energy in the range $E(i)$ to $E(i) + \Delta E$ where ΔE is the width of the energy bins. N_{theory} is the predicted fitting value for the number of particles in the energy range $E(i) + \Delta E$ using equation (4). The number of bins we are summing over, n, is determined by the number of bins from the simulated data, 200, and how far the fitted model extends beyond the data. Additional bins are added until the point at which the fit predicts zero particles. For bins beyond where there is simulation data, the number of simulated particles at that energy is zero.

References

[1] Jens Hjorth1 and Liliya L. R. Williams

STATISTICAL MECHANICS OF COLLISIONLESS ORBITS. I. ORIGIN OF CENTRAL CUSPS IN DARK-MATTER HALOS.

The Astrophysical Journal, 722:851855, 2010 October 10

[2] Navarro, Julio F., Carlos S. Frenk, and Simon D. M. White

The Structure of Cold Dark Matter Halos.

The Astrophysical Journal 462 (1996): 563-75.

[3] Einasto, J. and Haud, U.

Galactic Models with Massive Corona.

Astronomy and Astrophysics 223 (1989): 89-106

[4] Merritt, David, Navarro, Julio F., Ludlow, Aaron, and Jenkins, Adrian

A Universal Density Profile for Dark and Luminous Matter?.

The Astrophysical Journal 624 (2005): L85-L88

[5] J. F. Navarro, E. Hayashi, C. Power, A. R. Jenkins, C. S. Frenk, S. D. M. White, V. Springel, J. Stadel, and T. R. Quinn

The Inner Structure of ΛCDM haloes - III. Universality and asymptotic slopes.

Mon. Not. R. Astron. Soc 349 (2004): 1039-1051

[6] Leandro J. Beraldo e Silva, Marcos Lima, and Laerte Sodr Jr.

Testing phenomenological and theoretical models of dark matter density profiles with galaxy clusters.

Mon. Not. R. Astron. Soc (2013) arXiv:1301.1684

[7] Mike, Boylan-Kolchin.

Resolving Cosmic Structure Formation with the Millennium-II Simulation.

http://www.mpa-garching.mpg.de/galform/millennium-II/

[8] Springel, Volker and White, Simon D.M. and Jenkins, Adrian and Frenk, Carlos S. and Yoshida, Naoki et al.

Simulating the joint evolution of quasars, galaxies and their large-scale distribution

Nature 435 (2005)

[9] Volker Springel, Naoki Yoshida, Simon D.M. White

GADGET: a code for collisionless and gasdynamical cosmological simulations

New Astronomy 6 (2001): 79-117

[10] Volker Springel

The cosmological simulation code GADGET-2

Mon. Not. R. Astron. Soc. (2008) arXiv:astro-ph/0505010v1